2003

Collapse of Spatiotemporal Chaos

Renate Wackerbauer

Kenneth Showalter

Collapse of Spatiotemporal Chaos

Renate Wackerbauer[1] and Kenneth Showalter[2]
[1]Department of Physics, University of Alaska, Fairbanks, Alaska 99775-5920, USA
[2]Department of Chemistry, West Virginia University, Morgantown, West Virginia 26506-6045, USA
(Received 2 June 2003; published 22 October 2003)

The transient nature of spatiotemporal chaos is examined in reaction-diffusion systems with coexisting stable states. We find the apparent asymptotic spatiotemporal chaos of the Gray-Scott system to be transient, with the average transient lifetime increasing exponentially with medium size. The collapse of spatiotemporal chaos arises when statistical spatial correlations produce a quasihomogeneous medium, and the system obeys its zero-dimensional dynamics to relax to its stable asymptotic state.

DOI: 10.1103/PhysRevLett.91.174103 PACS numbers: 05.45.Jn, 05.45.Pq, 82.40.Bj, 89.75.Fb

The asymptotic stability of chaotic behavior in distributed systems is difficult to determine because transient spatiotemporal chaos may be extremely long lived. Spatiotemporal chaos has been found to be transient in a number of different types of distributed systems; however, a mechanistic understanding of the behavior remains elusive. In contrast, transient chaos in low-dimensional systems, in which a chaotic repellor is known to play an integral role in the behavior, is now well understood [1]. The abrupt change in complexity that is characteristic of transient spatiotemporal chaos, when a transition from chaotic to steady state or periodic behavior suddenly occurs, takes place in the absence of external perturbations. Transient spatiotemporal chaos has been suggested as an explanation for species extinction in ecological systems [2,3], and it has been studied in models for semiconductor charge transport [4] and for CO oxidation on single-crystal Pt surfaces [5,6]. Chaoslike spatiotemporal dynamics (with a negative maximum Lyapunov exponent) was also found to be transient in a system of coupled one-dimensional maps [7–9]. Transient spatiotemporal chaos typically exhibits an exponential increase in lifetime with increasing medium size [4,6,8,10], with the behavior generated by local information production and/or nonlinear transport properties [11,12].

In this Letter, we report on the transient nature of spatiotemporal chaos in the two-variable, Gray-Scott reaction-diffusion system. We characterize the transient dynamics and discuss how the behavior is related to other examples of transient spatiotemporal chaos.

The two-variable Gray-Scott model [13] describes an open, autocatalytic reaction: $A + 2B \rightarrow 3B$ and $B \rightarrow C$, where A represents the reactant, B the autocatalytic species, and C the final product. In a one-dimensional medium, the governing reaction-diffusion equations take the form [14]

$$\begin{aligned} \frac{\partial a}{\partial t} &= \delta \frac{\partial^2 a}{\partial x^2} + 1 - a - \mu a b^2, \\ \frac{\partial b}{\partial t} &= \frac{\partial^2 b}{\partial x^2} + b_0 - \Phi b + \mu a b^2, \end{aligned} \tag{1}$$

where a and b are the dimensionless concentrations of A and B, and Φ and μ are the bifurcation parameters, determined by the rate constants and concentration of reactant in the reservoir. Throughout this study, we assume equal diffusivities, $\delta = D_A/D_B = 1$, and, for simplicity, no supply of autocatalyst from the reservoir, $b_0 = 0$.

The spatially uniform (or zero-dimensional) system is characterized by three steady states: a stable node, $S^n = (1, 0)$, which exists for all parameter values, an unstable focus, $S^f = ((1 - \sqrt{1 - 4\Phi^2/\mu})/2, (1 + \sqrt{1 - 4\Phi^2/\mu})/(2\Phi))$, and a saddle point, $S^s = ((1 + \sqrt{1 - 4\Phi^2/\mu})/2, (1 - \sqrt{1 - 4\Phi^2/\mu})/(2\Phi))$, which exist for μ above the saddle node bifurcation, $\mu_{sn} = 4\Phi^2$. In the range $2 < \Phi < 4$, S^f becomes a stable focus for $\mu > \mu_H$, the subcritical Hopf bifurcation point, $\mu_H = \Phi^4/(\Phi - 1)$. The Hopf bifurcation point, μ_H, together with the critical threshold for traveling wave solutions, μ_c, determines the parameter range $[\mu_c, \mu_H]$ for wave-induced spatiotemporal chaos [14,15], with $\mu_c \approx 33$ for $\Phi = 2.8$.

The spatiotemporal behavior of Eqs. (1) has been analyzed in terms of a phase space description of the homogeneous (ordinary differential equation) system and the traveling wave (partial differential equation) system [14–16], revealing a heteroclinic connection from the unstable focus S^f to the stable node S^n for the former and a heteroclinic connection from S^n to S^f for the latter. The spatiotemporal chaos is described by a Šilnikov-like orbit [17], where the system spirals away from the unstable focus toward the stable node, only to be reinjected to the unstable focus via the propagating reaction-diffusion front.

The spatiotemporal dynamics is chaotic, with a rapid decay of spatial correlations [14] and a positive largest Lyapunov exponent [18]. The propagation of a localized disturbance in the chaotic medium was measured to characterize the intrinsic *damage spreading* by comparing the spatiotemporal behavior to that in an identical unperturbed system. We found no difference between the propagation velocities for moderately large to very small

(approaching infinitesimal) disturbances. The independence of the propagation velocity on perturbation magnitude points to a predominantly linear spatial information transmission process according to the classification scheme pursued in Refs. [11,12].

Figure 1 illustrates the transient nature of the spatiotemporal chaos. After a regime of sustained spatiotemporal chaos, a sudden, spontaneous transition takes place to the homogeneous, stable steady state. The higher temporal resolution shown in the lower panels of Fig. 1 does not yield an obvious interpretation for the abrupt extinction process.

A statistical analysis of the transient lifetime T_e for 100 randomly chosen initial distributions of species B reveals

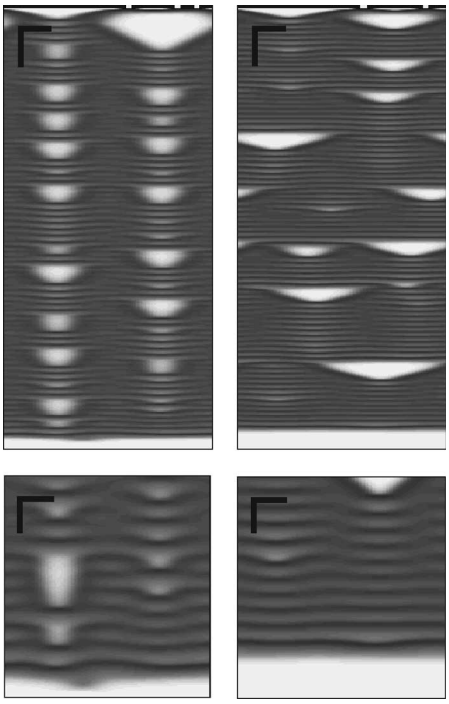

FIG. 1. Spatiotemporal pattern of reactant concentration a for $\Phi = 2.8$, $\mu = 33.2$ (left), and $\mu = 33.7$ (right). A concentration of 1(0) is represented in white (black), and time increases from top to bottom in each panel. Reactant A is initially distributed homogeneously, $a = 1$, over the entire domain of length $L = 30$. Species B is randomly seeded, indicated by the white rectangles in the top left and right panels, with a seed length of 0.75, an initial concentration of $b = 1$, and the constraint that at least two seeds are separated by a minimum length of 15. Both realizations of initial conditions have similar extinction times, $T_e = 409.7$ (left) and $T_e = 401.7$ (right). The upper panels are calculated for a total simulation time of $T = 420$, where the vertical bars represent 40 time units and the horizontal bars 5 space units. The extinction process during the last 15% of the simulation is shown in the corresponding lower panels, with a fivefold increase in temporal resolution, with the vertical bars representing 10 time units. An explicit Euler method ($\delta t = 0.0003$), with a three-point approximation of the Laplacian operator ($\delta x = 0.25$), and periodic boundary conditions were used for the numerical integration of the one-dimensional array.

an exponential increase of the average transient lifetime $\langle T_e \rangle_{100}$ with medium size N, Fig. 2(a). For each medium size, the frequency distribution of T_e follows an exponential decay. We find the values of $\langle T_e \rangle_{100}$ to be significantly larger for no-flux boundary conditions than for periodic boundary conditions [20]. The statistical robustness of the average transient lifetime $\langle T_e \rangle$ was demonstrated in control simulations with varying numerical precision, and when the number of simulations per medium size was increased to 2000, $\langle T_e \rangle$ changed by only 0.1% for $N = 120$.

Within the parameter range of spatiotemporal chaos, the average transient lifetime $\langle T_e \rangle_{100}$ depends exponentially on the parameter μ, limited from above by the Hopf bifurcation ($\mu_H = 34.15$ for $\Phi = 2.8$) and from below by the disappearance of traveling wave solutions ($\mu_c \approx 33$), Fig. 2(b). Close to the wave propagation threshold μ_c, $\mu = 33.15$, an increase in lifetime of the local extinctions results in a sharp increase in the average transient lifetime $\langle T_e \rangle_{100}$.

The extinction process is the consequence of statistical correlations in the medium such that a quasihomogeneous state is generated. In this quasihomogeneous state, the perturbations that normally initiate reaction-diffusion fronts, taking the system back to the unstable focus, are subthreshold and, hence, unable to sustain the spatiotemporal chaos. The corresponding trajectories throughout the medium closely follow the heteroclinic connection

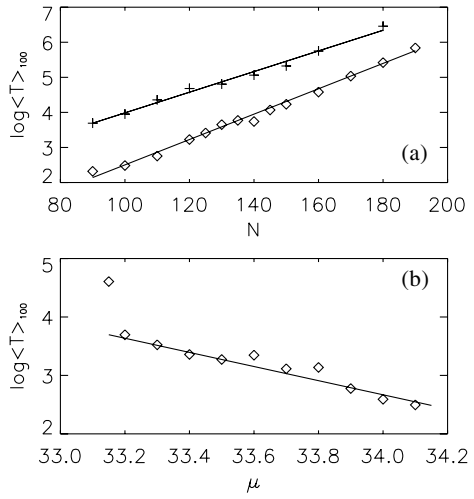

FIG. 2. (a) Average transient lifetime as a function of medium length (in grid points) for periodic (◇) and no-flux (+) boundary conditions. Each average value was determined from 100 realizations with random initial seed distributions. All of the parameters are the same as in Fig. 1 with $\mu = 33.7$. The full lines show "robust least absolute deviation" fits of the average transient lifetimes. (b) Average transient lifetime (◇) as a function of the parameter μ for periodic boundary conditions and a medium of length $L = 30$ ($N = 120$). The full line shows the best linear fit within the parameter range $\mu \in [33.2, 34.1]$. The fitting procedure, averaging, and other parameters are the same as in (a) [19].

from the unstable focus S^f to the stable node S^n [14], and the system reaches its stable, spatially homogeneous asymptotic state.

Figure 3(a), shows the temporal dynamics of the reactant concentration a at three equally spaced locations, illustrating the transition to spatially correlated behavior. There is little evidence of correlation until $t \approx 390$, when the three time series suddenly become virtually identical to approach the extinction at $t = 401.7$ [21]. Figure 3(b) shows that the average distance d_0 of the trajectories in phase space, $d_0(t) = \sum_{i=1}^{N-1} \sqrt{(a_i(t) - a_0(t))^2 + (b_i(t) - b_0(t))^2}\,/(N-1)$, approaches zero in the quasihomogeneous medium prior to the extinction.

Spatially localized regions of extinction, shown as white pulses in Fig. 1 and $a \approx 1$ in Fig. 3(a), continually appear during the system evolution; however, these regions are bounded and consumed by reaction-diffusion fronts. Hence, the localized regions of extinction continually decrease in size and are unable to merge to form larger scale extinctions. Figure 3(b) shows that the maximum autocatalyst concentration in the medium at any given time, $b_m(t) = \max\{b_i(t)\}_{0 \le i \le N-1}$, remains above the value observed in the local extinctions, reflecting the presence of the reaction-diffusion fronts taking the system back to the unstable focus. However, before the global extinction at $t \approx 390$, b_m drops dramatically and approaches zero.

If the statistical correlation of the spatiotemporal behavior is prevented, no collapse can occur and asymptotic spatiotemporal chaos is exhibited. Figure 4(a) shows asymptotic chaotic behavior resulting from imposed constant boundary conditions, $a = 0.4, b = 0.3$, at the right-hand side of the medium. This boundary condition prevents the occurrence of a global extinction because it provides a continuous perturbation in the form of reaction-diffusion fronts that take the system from the extinct state S^n back to the unstable focus S^f [22].

The exponential increase in average transient time $\langle T_e \rangle_{100}$ with medium size suggests that a basin of *spatiotemporal configurations*, achieved statistically, leads to the global extinction and collapse of spatiotemporal chaos. Following studies of escape statistics of chaotic repellers in low-dimensional transient chaos [1], we construct sets of quasihomogeneous media, where all trajectories have either the same initial distance to the unstable focus or the same initial phase, and determine the basin of spatiotemporal configurations for immediate escape to the stable node. A typical escape distribution is shown in

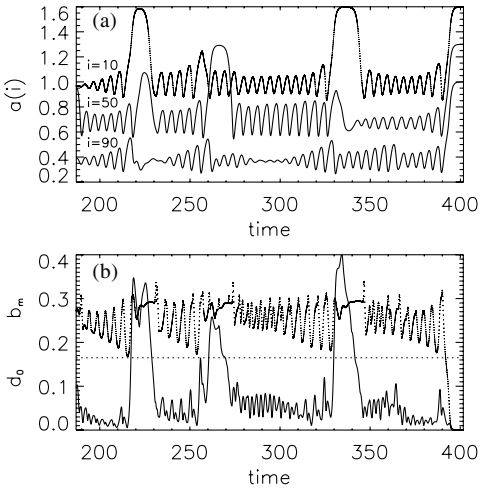

FIG. 3. (a) Time series of reactant concentration a at three equally spaced locations in the medium ($i = 10, 50, 90$) for the simulation in Fig. 1 (right panel). For clarity, the middle and upper curves are offset vertically by 0.3 and 0.6, respectively. (b) The maximum concentration of B, b_m (dotted line), and the average distance of the trajectories in phase space, d_0 (full line), as a function of time for the simulation in (a). The horizontal line is to guide the eye in comparing the minima in b_m.

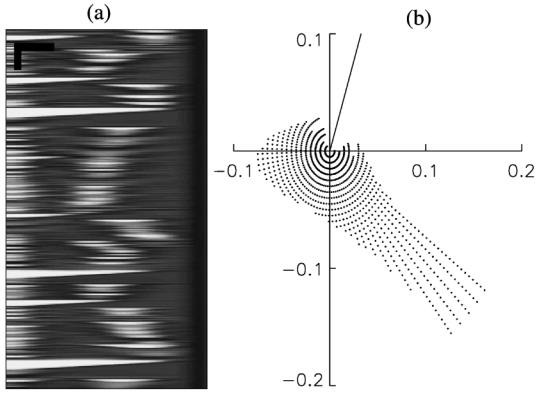

FIG. 4. (a) Spatiotemporal dynamics of the reactant concentration a ($\mu = 33.2$) for a time interval of 3100 and a temporal resolution of 1.5. No-flux boundary conditions were used on the left-hand side and Dirichlet boundary conditions ($a = 0.4, b = 0.3$) on the right-hand side (medium length $L = 25$). The horizontal and vertical bars represent 5 space and 200 time units, respectively. (b) Distribution of initial conditions that give rise to immediate extinction (white) or immediate survival (black) of spatiotemporal chaos for different quasihomogeneous states. The origin of the coordinate system is at the unstable focus S^f; the stable node S^n is located at $(0.63, -0.23)$. The plot was constructed by carrying out multiple simulations, with each simulation having all trajectories at the same initial distance r_0 from the origin but with a fraction of the trajectories differing in phase from the others. The initial phase of 285 neighboring trajectories was $n\pi/5$, indicated by the radial line, while the phase Φ_0 of the remaining 15 trajectories was varied in steps of $\pi/50$ in successive simulations. This sequence was repeated with the distance r_0 increased in steps of 0.005 until the region $r_0 \le 0.2$, Φ_0 was mapped. Each initial condition was marked with a dot when the quasihomogeneous medium survived the first approach to the stable node. Ten distributions were determined with $n = 1, \ldots, 10$; the distribution for $n = 2$ is shown. Medium size $N = 300$ and $\mu = 33.7$; other parameters are the same as in Fig. 1.

Fig. 4(b), which reveals phase relations that favor either immediate extinction or immediate survival. For a given dominant phase of the quasihomogeneous medium, shown by the radial line, particular phase relationships of neighboring trajectories favor survival, reflected by the tail-like dotted structure, whereas other phase relationships favor extinction, reflected by the white sector aligned with the dominant phase. A total of ten distributions with varying dominant phases were calculated, and each revealed a unique escape pattern. All distributions, however, showed the common feature of a sector aligned along the dominant phase favoring extinction, corresponding to the quasihomogeneous medium.

In summary, the collapse of spatiotemporal chaos in Eqs. (1) is initiated by statistical spatial correlations, yielding a quasihomogeneous state that evolves to the stable asymptotic state of the system, the stable node S^n. The transient nature of spatiotemporal chaos in systems with an accessible globally stable (steady or periodic) state appears in other systems. We find a similar quasihomogeneous state leading to the collapse of spatiotemporal chaos in the 1D Bär-Eiswirth model [5], a realistic model for the oxidation of CO on Pt. The transient nature of 2D spiral turbulence in this system has been reported by Greenside and co-workers [6].

The transient spatiotemporal chaos in the Gray-Scott model further complements the classification scheme of irregular spatiotemporal dynamics pursued in Refs. [11,12]. We find a positive maximum Lyapunov exponent in this system, much like that found in models for semiconductor charge transport [4]. We also find propagation velocities of localized disturbances to be independent of the perturbation size. This is in contrast to the chaotic behavior found in coupled one-dimensional maps [8,9], which exhibits a negative maximum Lyapunov exponent and, hence, arises from nonlinear transport properties rather than local information production. We expect the collapse of spatiotemporal chaos in these different types of systems to occur by the same mechanism, despite the differences in their chaotic dynamics, since they all exhibit globally stable (steady or periodic) states that can be realized via a quasihomogeneous medium [23].

While we are certain that local extinctions do not merge to give rise to the global extinction, we know less about the possible synchronization of neighboring regions near the unstable focus S^f. The decrease in average transient lifetime $\langle T_e \rangle_{100}$ with increasing μ, Fig. 2(b), suggests some degree of synchronization, since the system spends more time near the unstable focus as the value of μ approaches the Hopf bifurcation. Hence, as the focus becomes less strongly repelling, neighboring regions have more time to diffusively interact and synchronize.

K. S. thanks the National Science Foundation (CHE-9974336) and the Office of Naval Research (N00014-01-1-0596) and R.W. thanks the University of Alaska Fairbanks for supporting this research.

[1] C. Grebogi, E. Ott, and J. A. Yorke, Physica (Amsterdam) **7D**, 181 (1983); T. Tel, in *Directions in Chaos III*, edited by H. Bai-lin (World Scientific Publishing, Singapore, 1990), pp. 149–211.
[2] K. McCann and P. Yodzis, Am. Nat. **144**, 873 (1994).
[3] L. Shulenburger, Y.-C. Lai, T. Yalcinkaya, and R. D. Holt, Phys. Lett. A **260**, 156 (1999).
[4] A. Wacker, S. Bose, and E. Schöll, Europhys. Lett. **31**, 257 (1995).
[5] M. Bär and M. Eiswirth, Phys. Rev. E **48**, R1635 (1993).
[6] M. C. Strain and H. S. Greenside, Phys. Rev. Lett. **80**, 2306 (1998).
[7] J. P. Crutchfield and K. Kaneko, Phys. Rev. Lett. **60**, 2715 (1988).
[8] A. Politi, R. Livi, G. L. Oppo, and R. Kapral, Europhys. Lett. **22**, 571 (1993).
[9] R. Kapral, R. Livi, G. L. Oppo, and A. Politi, Phys. Rev. E **49**, 2009 (1994).
[10] K. Kaneko, Phys. Lett. A **149**, 105 (1990).
[11] A. Politi and A. Torcini, Europhys. Lett. **28**, 545 (1994).
[12] M. Cencini and A. Torcini, Phys. Rev. E **63**, 056201 (2001).
[13] P. Gray and S. K. Scott, Chem. Eng. Sci. **39**, 1087 (1984).
[14] J. H. Merkin, V. Petrov, S. K. Scott, and K. Showalter, Phys. Rev. Lett. **76**, 546 (1996); J. Chem. Soc. Faraday Trans. **92**, 2911 (1996).
[15] J. H. Merkin and M. A. Sadiq, IMA J. Appl. Math. **57**, 273 (1996).
[16] Y. Nishiura and D. Ueyama, Physica D (Amsterdam) **150**, 137 (2001).
[17] L. P. Šilnikov, Sov. Math. Dokl. **6**, 163 (1965); **8**, 54 (1967).
[18] The largest Lyapunov exponent ($\lambda_{\max} \approx 0.08$ for $\mu = 33.7$) was numerically determined in a $2N$-dimensional phase space, where N is the number of spatial grid points [G. Benettin, L. Galgani, and J. M. Strelcyn, Phys. Rev. A **14**, 233 (1976)].
[19] In a few simulations, the chaotic spatiotemporal dynamics transformed into a stationary pattern. This asymptotic state appeared for 4 out of the 100 initial conditions when $\mu = 33.15$. A single realization for $\mu = 33.4$ resulted in a spatiotemporal periodic asymptotic state rather than the extinct state S^n. The corresponding transient lifetimes are not shown in Fig. 2(b).
[20] An apparent enhancement of local extinctions at the boundary with no-flux boundary conditions [14] gives rise to longer transient lifetimes because local extinctions inhibit the global extinction (see discussion).
[21] Some global extinctions occurred as phase waves, with distinct phase lags between the three trajectories at equally spaced locations.
[22] A self-segregation interface that develops when n identical species compete for a common resource plays a similar role in preventing extinction in an $(n + 1)$-variable system analogous to Eqs. (1) [R. Wackerbauer, H. Sun, and K. Showalter, Phys. Rev. Lett. **84**, 5018 (2000)].
[23] We note that recent studies of chaotic maps on fractal networks indicate that topology may play a decisive role in determining asymptotic collective behaviors [K. Tucci, M. G. Cosenza, and O. Alvarez-Llamoza, Phys. Rev. E **68**, 027202 (2003)].